

# Experimental study of perpendicular transport in weakly coupled $\text{Al}_x\text{Ga}_{1-x}\text{N}/\text{GaN}$ superlattices

E. L. Waldron,<sup>a)</sup> Y.-L. Li, and E. F. Schubert<sup>b)</sup>

Department of Electrical, Computer, and Systems Engineering, 110 Eighth Street, Rensselaer Polytechnic Institute, Troy, New York 12180

J. W. Graff

Electrical and Computer Engineering Department, 8 Saint Mary's Street, Boston University, Boston, Massachusetts 02155

J. K. Sheu

Optical Science Center, National Central University, Chung-Li 32054, Taiwan, Republic of China

(Received 30 June 2003; accepted 8 October 2003)

Perpendicular transport characteristics of  $n$ -type  $\text{Al}_x\text{Ga}_{1-x}\text{N}/\text{GaN}$  superlattices are presented. Planar and mesa-etched superlattice structures are employed to identify the perpendicular resistance. Perpendicular transport measurements in  $\text{Al}_{0.22}\text{Ga}_{0.78}\text{N}/\text{GaN}$  superlattices display linear current–voltage characteristics with a resistivity that is a factor of 6.6 higher than for bulk material. A theoretical model is developed for perpendicular transport in  $\text{Al}_x\text{Ga}_{1-x}\text{N}/\text{GaN}$  superlattices based on sequential tunneling. The model shows that short superlattice periods are required to minimize the perpendicular resistivity. © 2003 American Institute of Physics. [DOI: 10.1063/1.1631382]

Efficient perpendicular transport (electrical transport along growth direction) in  $\text{Al}_x\text{Ga}_{1-x}\text{N}/\text{GaN}$  superlattices (SLs) is critical to the operation of many AlGaIn-based devices, including heterobipolar transistors, light-emitting diodes, and laser diodes where SLs are used for enhanced doping activation<sup>1–3</sup> and reduction of line defect density.<sup>4</sup> It is well known that doped SLs<sup>5</sup> alleviate the problem of large activation energy ( $\sim 200$  meV) in  $p$ -type GaN and related compounds. However, there has been little research on perpendicular transport in  $\text{Al}_x\text{Ga}_{1-x}\text{N}/\text{GaN}$  SLs.

In this letter, we analyze perpendicular transport in  $n$ -type  $\text{Al}_x\text{Ga}_{1-x}\text{N}/\text{GaN}$  SLs and bulk GaN both experimentally and theoretically. For the determination of the perpendicular and in-plane resistivities in  $n$ -type  $\text{Al}_{0.22}\text{Ga}_{0.78}\text{N}/\text{GaN}$  SLs, a modified transfer length method (TLM) is used. The results are explained in terms of a theoretical model based on sequential tunneling and free carrier concentration enhancement.

The Ga-faced  $\text{Al}_{0.22}\text{Ga}_{0.78}\text{N}/\text{GaN}$  SLs were grown by metalorganic chemical vapor deposition on  $c$ -plane sapphire substrates. The  $\text{Al}_{0.22}\text{Ga}_{0.78}\text{N}/\text{GaN}$  SLs are uniformly doped with Si at a level of  $5 \times 10^{17} \text{ cm}^{-3}$  and are grown on bulk  $n$ -type GaN. The bulk  $n$ -type GaN is  $4.0 \mu\text{m}$  thick and is also uniformly Si doped at  $5 \times 10^{17} \text{ cm}^{-3}$ . The SL is  $0.3 \mu\text{m}$  thick, has 30 periods, and equal well and barrier widths of  $50 \text{ \AA}$ . Standard photolithographic techniques and argon-ion etching were employed to create mesa patterns.  $200 \mu\text{m} \times 100 \mu\text{m}$  Ti/Al/Ni/Au contacts, annealed at  $800^\circ\text{C}$  for 30 s in an  $\text{N}_2$  ambient, were deposited using electron-beam evaporation. All contacts showed linear current–voltage characteristics.

Figure 1 shows a typical TLM measurement and a schematic of the  $\text{Al}_{0.22}\text{Ga}_{0.78}\text{N}/\text{GaN}$  SL. The typical measured specific contact resistivity is  $2.6 \times 10^{-4} \Omega \text{ cm}^2$ . Figure

2(a) shows the TLM measurement and a schematic of the SL after the initial etch. Extrapolating the inter-TLM contact separation,  $L_c$ , to zero yields the total resistance of the structure, given by  $R_{\text{total}} = 2R_c + 2R_{\text{SL}} + 2R_{\text{bulk}}$ , where  $R_c$  is the contact resistance,  $R_{\text{SL}}$  is the perpendicular resistance of the SL, and  $R_{\text{bulk}}$  is the perpendicular resistance bulk GaN. In the limit  $L_c \rightarrow 0$ , the lateral resistance between the two mesas vanishes. The resistances  $R_{\text{SL}}$  and  $R_{\text{bulk}}$  are given by

$$R_{\text{SL}} = \rho_{\text{SL}} \frac{d_{\text{SL}}}{A}, \quad \text{and} \quad R_{\text{bulk}} = \rho_{\text{bulk}} \frac{d_{\text{bulk}}}{A}, \quad (1)$$

respectively. In Eq. (1),  $\rho_{\text{SL}}$  is the perpendicular resistivity of the SL,  $d_{\text{SL}} = 0.3 \mu\text{m}$  is the thickness of the SL defined by the mesa,  $A = 2 \times 10^{-4} \text{ cm}^2$  is the area of the mesa,  $\rho_{\text{bulk}}$  is the perpendicular resistivity of the bulk GaN, and  $d_{\text{bulk}} = d - d_{\text{contact}} - d_{\text{SL}}$  is the height of the bulk GaN defined by the mesa with  $d$  being the total height of the mesa. Thus, having measured  $R_{\text{total}}$  for different values of  $d_{\text{bulk}}$ , we can determine the values of  $\rho_{\text{SL}}$  and  $\rho_{\text{bulk}}$ .

The mesa structure shown in Fig. 2(a) has a value of  $d_{\text{bulk}} = 0.37 \mu\text{m}$ . The mesa structure shown in Fig. 2(b) has a

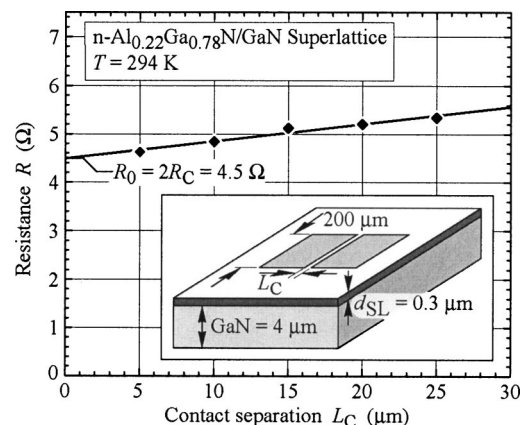


FIG. 1. TLM measurement and schematic sample structure of unetched  $n$ -type  $\text{Al}_{0.22}\text{Ga}_{0.78}\text{N}/\text{GaN}$  superlattice.

<sup>a)</sup>Present address: The Charles Stark Draper Laboratory, 555 Technology Square, Cambridge, Massachusetts 02139.

<sup>b)</sup>Electronic mail: efschubert@rpi.edu

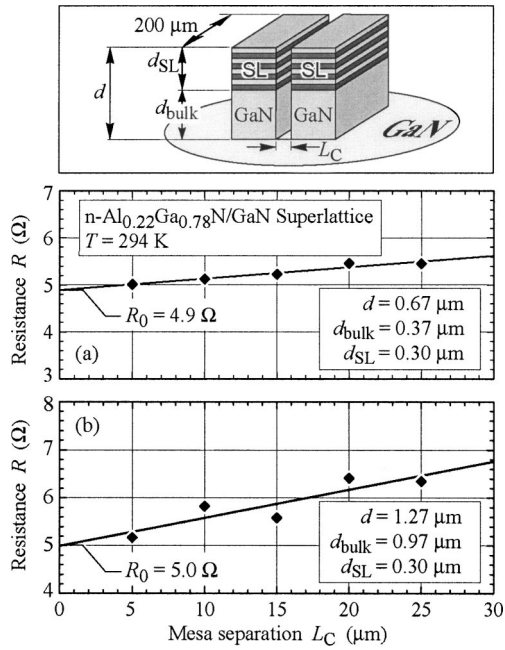


FIG. 2. TLM measurements on  $n$ -type  $\text{Al}_{0.22}\text{Ga}_{0.78}\text{N}/\text{GaN}$  superlattices used for analysis of perpendicular transport for bulk layer thicknesses ( $d_{\text{bulk}}$ ) of (a)  $0.37 \mu\text{m}$  and (b)  $0.97 \mu\text{m}$ . Also shown is the schematic sample structure.

value of  $d_{\text{bulk}} = 0.97 \mu\text{m}$ . Using these data in Eq. (1) yields  $\rho_{\text{SL}} = 1.2 \Omega \text{ cm}$  and  $\rho_{\text{bulk}} = 0.18 \Omega \text{ cm}$  for the perpendicular resistivities of the  $\text{Al}_{0.22}\text{Ga}_{0.78}\text{N}/\text{GaN}$  SL and bulk GaN, respectively. Thus, the perpendicular resistivity is a factor of 6.6 higher than the bulk resistivity.

We next develop a theoretical model for perpendicular transport in  $\text{Al}_x\text{Ga}_{1-x}\text{N}/\text{GaN}$  SLs. The model is based on sequential tunneling of carriers through the barriers and the carrier concentration enhancement occurring in doped SLs. The theoretical model shows that the design parameters of  $\text{Al}_x\text{Ga}_{1-x}\text{N}/\text{GaN}$  SLs can be chosen in a way that maximizes the conductivity even along the perpendicular direction of the SL. Note that negative differential resistivity (NDR) in the current–voltage data is not observed. Such NDR has been reported in literature.<sup>6,7</sup>

The low-field current density in bulk material is given by  $J = env = en\mu F$ , where  $e$ ,  $n$ ,  $v$ ,  $\mu$ , and  $F$  are the magnitude of the electronic charge, the carrier concentration, the carrier drift velocity, the mobility, and the applied electric field, respectively. The conductivity in bulk material is given by  $\sigma = en\mu$ . Thus, the conductivity is determined by two material parameters, namely carrier concentration and mobility. We next discuss transport in SLs and show that transport is determined by the carrier concentration and a tunneling parameter.

The self-consistently calculated band diagram and ground-state wave functions of an  $\text{Al}_{0.22}\text{Ga}_{0.78}\text{N}/\text{GaN}$  SL are shown in Fig. 3(a) without an external electric field. Figure 3(b) shows a schematic of the band diagram with an external field. The conduction-band discontinuity of the two semiconductors forming the SL is assumed to be  $\Delta E_C$ . The SL is assumed to have a well layer thickness of  $L_{\text{QW}}$ , a barrier layer thickness of  $L_B$ , and a SL period of  $L_{\text{SL}} = L_{\text{QW}} + L_B$ . Carriers within the well layers are quantized for motion along the perpendicular direction of the SL and the quantized ground-state energy is denoted by  $E_0$ .

Figure 3 also shows that under bias conditions, carriers

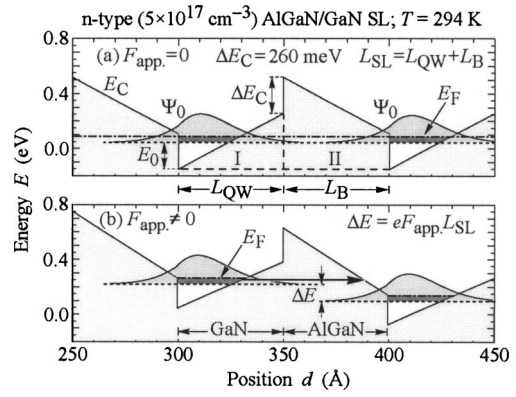


FIG. 3. (a) Self-consistently calculated band diagram at 300 K and ground-state wave functions of uniformly doped  $n$ -type  $\text{Al}_{0.22}\text{Ga}_{0.78}\text{N}/\text{GaN}$  superlattice ( $N_D = 5 \times 10^{17} \text{ cm}^{-3}$ ) with no external electric field applied. (b) Schematic of  $\text{Al}_{0.22}\text{Ga}_{0.78}\text{N}/\text{GaN}$  superlattice band diagram with an external electric field applied.

can tunnel from one quantum well to empty states in an adjacent quantum well. Using the attempt-to-escape model, the current density in SLs can be written as

$$J = env = en_{\text{ava}}^{2\text{D}} \tau^{-1}, \quad (2)$$

where  $v$  denotes the average drift velocity of electrons propagating in the superlattices,  $n_{\text{ava}}^{2\text{D}}$  is the two-dimensional carrier density available for tunneling, i.e., the density of carriers that can tunnel to an adjacent quantum well, and  $\tau$  is the mean time a carrier resides in one quantum well before tunneling to the adjacent quantum well. For carriers to be available for tunneling, it is required that empty states at the same energy be available in the adjacent quantum well. The available carrier density is then given by

$$n_{\text{ava}}^{2\text{D}} = \rho_{\text{DOS}}^{2\text{D}} \Delta E = \rho_{\text{DOS}}^{2\text{D}} e F L_{\text{SL}}, \quad (3)$$

where  $\Delta E$  is the energy drop between two adjacent quantum wells under bias conditions. Equation (3) assumes the high-degeneracy approximation, in which the Fermi distribution is taken to be a steplike function. The energy drop,  $\Delta E$ , is related to the external bias,  $V$ , by  $\Delta E = eV/(\text{number of SL periods})$ . The validity of Eq. (3) is restricted to

$$n^{2\text{D}} > \rho_{\text{DOS}}^{2\text{D}} \Delta E, \quad (4)$$

where  $n^{2\text{D}}$  is the carrier concentration per  $\text{cm}^2$  in one quantum well, that is,  $(E_F - E_0) > \Delta E$ . Equation (4) shows that the 2D carrier concentration has a minimum and cannot be arbitrarily small. This restriction should not be problematic if (i) carrier concentrations in SLs are high and (ii) the potential drop per period is small. For example, in our  $\text{Al}_{0.22}\text{Ga}_{0.78}\text{N}/\text{GaN}$  SL data, the experimental maximum voltage applied never exceeded  $\sim 0.5 \text{ V}$ . Applying this voltage over the TLM structure yields an energy drop per period of  $\sim 1 \text{ meV}$  ( $\sim 450 \text{ mV}$  over contacts,  $\sim 50 \text{ mV}$  over 60 SL periods). Thus, the validity of the model can be considered to be limited to small bias values. At such small bias values, Eq. (4) is satisfied.

The time  $\tau$  given in Eq. (2) is the mean time a carrier resides in one quantum well before tunneling to the adjacent quantum well. This time is given by

$$\tau = \frac{2L_{\text{QW}}}{v} T^{-1} = \frac{2L_{\text{QW}}}{\sqrt{2E_0/m^*}} T^{-1}, \quad (5)$$

where  $T$  is the tunneling probability through the barrier and  $m^*$  is the carrier effective mass ( $m^* = 0.2 m_0$  for electrons in GaN). In Eq. (5), it is assumed that the quantum energy  $E_0$  is purely kinetic. This is correct for an infinite square well and is a reasonable approximation for deep wells.

We assume that the magnitude of the bias is so small that the shape of the barrier is not significantly altered, as compared to the no-bias case. This allows us to use a triangular and trapezoidal barrier model for the tunneling probability, depicted in Fig. 3(a) as regions I and II, respectively. The tunneling probability through the triangular region I is given by

$$T_1 = \exp\left(\frac{-4\sqrt{2m^*}}{3eF\hbar}(V_0^I - E_0)^{3/2}\right), \quad (6)$$

where  $V_0^I = eFL_{QW}$  and the ground-state energy in the well is given by<sup>8</sup>

$$E_0 = \left(\frac{3}{16} \frac{ehF_{\text{pol}}}{\sqrt{2m^*}}\right)^{2/3}, \quad (7)$$

where  $h$  is Planck's constant and  $F_{\text{pol}}$  is the internal electric field, which for simplicity we consider due only to the polarization effects.<sup>9</sup> The tunneling probability through the trapezoidal region II is given by

$$T_{II} = \exp\left(\frac{-4\sqrt{2m^*}}{3eF\hbar}[(V_0^{II} - E_0)^{3/2} - (V_0^{II} - E_0 - eFL_B)^{3/2}]\right), \quad (8)$$

where  $V_0^{II} = V_0^I + \Delta E_c = eFL_{QW} + \Delta E_c$  and  $\Delta E_c = 260$  meV for  $x = 22\%$ .<sup>10</sup>

The total tunneling probability from one quantum well to an adjacent quantum well is given by  $T = T_1 \times T_{II}$ . Rewriting Eq. (2) using Eqs. (3) through (8) yields

$$J = \frac{e^2 \rho_{\text{DOS}}^{2D} L_{\text{SL}}}{2L_{\text{QW}}} \sqrt{\frac{2E_0}{m^*}} F \exp\left\{\frac{4\sqrt{2m^*}}{3eF\hbar}[(eF(L_{\text{QW}} - L_B) + \Delta E_c - E_0)^{3/2} - 2(eFL_{\text{QW}} - E_0)^{3/2}]\right\}. \quad (9)$$

Using  $J = \sigma_{\text{SL}} F$ , the conductivity along the perpendicular direction of the SL can be identified as

$$\begin{aligned} \sigma_{\text{SL}} &= \frac{e^2 \rho_{\text{DOS}}^{2D} L_{\text{SL}}}{2L_{\text{QW}}} \sqrt{\frac{2E_0}{m^*}} T \\ &= \frac{e^2 \rho_{\text{DOS}}^{2D} L_{\text{SL}}}{2L_{\text{QW}}} \sqrt{\frac{2E_0}{m^*}} \exp\left\{\frac{4\sqrt{2m^*}}{3eF\hbar}[(eF(L_{\text{QW}} - L_B) + \Delta E_c - E_0)^{3/2} - 2(eFL_{\text{QW}} - E_0)^{3/2}]\right\}. \end{aligned} \quad (10)$$

Inspection of Eq. (10) reveals that the SL conductivity is fundamentally different from bulk conductivity. Due to the powerful tunneling (exponential) term, it is necessary to keep the barrier layers sufficiently thin to enable a high tunneling probability and thus efficient perpendicular transport. A high carrier concentration is relevant for both superlattice as well as bulk transport.

The SL and bulk conductivity are shown in Fig. 4 as a function of the SL period. Figure 4 shows that the SL and

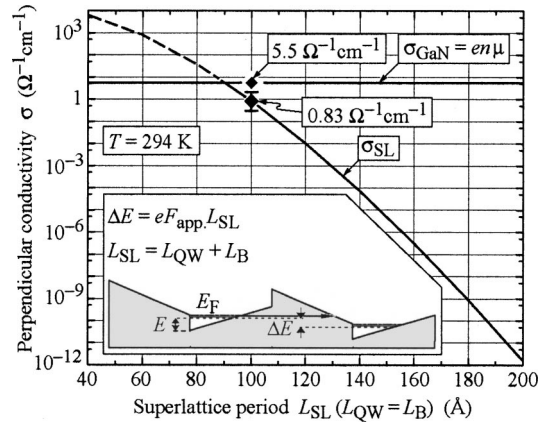


FIG. 4. Calculated perpendicular conductivity in  $n$ -type  $\text{Al}_{0.22}\text{Ga}_{0.78}\text{N}/\text{GaN}$  SL and bulk  $n$ -type GaN, both doped at  $5 \times 10^{17} \text{ cm}^{-3}$ . The data points are values obtained from experimental results.

bulk conductivities become increasingly similar for values of  $L_{\text{SL}} \leq 100 \text{ \AA}$ . In Fig. 4, an internal polarization field of  $F_{\text{pol}} = 6.7 \times 10^5 \text{ V/cm}$  was used. This field matched the  $\sigma_{\text{SL}}$  data very well. In addition, this value for  $F$  is in reasonable agreement with our self-consistently calculated value of  $F_{\text{pol}} = 8.0 \times 10^5 \text{ V/cm}$ .<sup>9</sup> The perpendicular conductivity depends strongly on  $F_{\text{pol}}$  because it appears in the exponential tunneling term [see Eq. (10)]. Using the self-consistently calculated  $F_{\text{pol}} = 8.0 \times 10^5 \text{ V/cm}$  would yield  $\sigma_{\text{SL}} = 0.12 \text{ \Omega}^{-1} \text{ cm}^{-1}$ . The error bar shown in Fig. 4 results from an error analysis that takes into account contact-to-contact sample-to-sample variations found in multiple measurements. For the GaN conductivity shown in Fig. 4,  $\sigma_{\text{GaN}}$ , a mobility of  $100 \text{ cm}^2/(\text{V s})$  and a donor activation energy of  $39 \text{ meV}$  were used.

In conclusion, the perpendicular resistivity in  $n$ -type  $\text{Al}_{0.22}\text{Ga}_{0.78}\text{N}/\text{GaN}$  SLs was determined and compared with bulk  $n$ -type GaN doped at the same level. The SL has a measured perpendicular resistivity of  $1.2 \text{ \Omega cm}$ , a factor of 6.6 higher than the bulk resistivity. A theoretical model based on sequential tunneling and free carrier concentration enhancement is developed to explain the results. The model demonstrates that the SL perpendicular transport is fundamentally different than the bulk transport.

This work was supported by ONR, DARPA, and NSF.

<sup>1</sup>E. L. Waldron, J. W. Graff, and E. F. Schubert, Appl. Phys. Lett. **79**, 2737 (2001).

<sup>2</sup>I. D. Goepfert, E. F. Schubert, A. Osinsky, P. E. Norris, and N. N. Faleev, J. Appl. Phys. **88**, 2030 (2000).

<sup>3</sup>P. Kozodoy, Y. P. Smorchkova, M. Hansen, H. Xing, S. P. DenBaars, U. K. Mishra, A. W. Saxler, R. Perrin, and W. C. Mitchel, Appl. Phys. Lett. **75**, 2444 (1999).

<sup>4</sup>T. Wang, Y. H. Liu, Y. B. Lee, Y. Izumi, J. P. Ao, J. Bai, H. D. Li, and S. Sakai, J. Cryst. Growth **235**, 177 (2002).

<sup>5</sup>E. F. Schubert, W. Grieshaber, and I. D. Goepfert, Appl. Phys. Lett. **69**, 3737 (1996).

<sup>6</sup>L. Esaki and L. L. Chang, Phys. Rev. Lett. **33**, 495 (1974).

<sup>7</sup>A. Sibille, in *Semiconductor Superlattices*, edited by H. T. Grahn (World Scientific, Singapore, 1995), Chap. 2.

<sup>8</sup>The ground-state energy given by Eq. (11) is the solution of a symmetric V-shaped well using the Wentzel-Kramers-Brillouin approximation.

<sup>9</sup>O. Ambacher, J. Majewski, C. Miskys, A. Link, M. Hermann, M. Eickhoff, M. Stutzmann, F. Bernardini, V. Fiorentini, V. Tilak, B. Schaff, and L. F. Eastman, J. Phys.: Condens. Matter **14**, 3399 (2002).

<sup>10</sup> $\Delta E_c = 0.63 \times \Delta E_g$  with  $E_{g, \text{AlGaIn}}(x) = [3.42(1-x) + 6.13x - 1.0x(1-x)] \text{ eV}$ ,  $m_e = 0.2m_0$ .